Article type : Article (CPT)

Metamizole is a moderate cytochrome P450 inducer via the constitutive androstane receptor and a weak inhibitor of CYP1A2

Fabio Bachmann[1,2], Urs Duthaler[1,2], Henriette E. Meyer zu Schwabedissen[3], Maxim Puchkov[4], Jörg Huwyler[4], Manuel Haschke[5,6], Stephan Krähenbühl[1,2]

[1]Division of Clinical Pharmacology & Toxicology, University Hospital Basel, Switzerland

[2]Department of Biomedicine, University of Basel, Switzerland

[3]Biopharmacy, Department of Pharmaceutical Sciences, University of Basel, Switzerland

[4]Pharmaceutical Technology, Department of Pharmaceutical Sciences, University of Basel, Switzerland

[5]Clinical Pharmacology and Toxicology, Department of General Internal Medicine, Inselspital, Bern University Hospital, University of Bern, Switzerland

[6]Institute of Pharmacology, University of Bern, Switzerland

Corresponding author:

Stephan Krähenbühl, MD, PhD

Clinical Pharmacology & Toxicology, University Hospital Basel,4031 Basel, Switzerland

Phone: +41 61 265 47 15

Fax: +41 61 265 4560

E-mail: stephan.kraehenbuehl@usb.ch

This article has been accepted for publication and undergone full peer review but has not been through the copyediting, typesetting, pagination and proofreading process, which may lead to differences between this version and the Version of Record. Please cite this article as doi: 10.1002/CPT.2141

Conflict of interest: SK gave talks in symposia sponsored by Sanofi. All other authors declared no competing interests for this work.

Financial support: The study was supported by a grant from the Swiss National Science foundation to MH and SK (SNF 31003A_156270)

Key words: Metamizole, N-methyl-4-aminoantipyrine (4-MAA), CYP induction, CAR, PXR

Abstract

Metamizole is an analgesic and antipyretic drug used intensively in certain countries. Previous studies have shown that metamizole induces cytochrome (CYP) 2B6 and possibly CYP3A4. So far, it is unknown whether metamizole induces additional CYPs and by which mechanism. Therefore, we assessed the activity of 6 different CYPs in 12 healthy male subjects before and after treatment with 3 g of metamizole per day for one week using a phenotyping cocktail approach. In addition, we investigated whether metamizole induces CYPs by an interaction with the constitutive androstane receptor (CAR) or the pregnane X receptor (PXR) in HepaRG cells. In the clinical study, we confirmed a moderate induction of CYP2B6 (decrease in the efavirenz AUC by 79%) and 3A4 (decrease in the midazolam AUC by 68%) by metamizole. In addition, metamizole weakly induced CYP2C9 (decrease in the flurbiprofen AUC by 22%) and moderately CYP2C19 (decrease in the omeprazole AUC by 66%) but did not alter CYP2D6 activity. In addition, metamizole weakly inhibited CYP1A2 activity (1.79-fold increase in the caffeine AUC). We confirmed these results in HepaRG cells, where 4-MAA, the principal metabolite of metamizole, induced the mRNA expression of CYP2B6, 2C9, 2C19 and 3A4. In HepaRG cells with a stable knockout of PXR or CAR, we could demonstrate that CYP induction by 4-MAA depends on CAR and not on PXR. In conclusion, metamizole is a broad CYP inducer by an interaction with CAR and an inhibitor of CYP1A2. Regarding the widespread use of metamizole, these findings are of substantial clinical relevance.

Introduction

Metamizole (dipyrone) is an old drug with analgesic, antipyretic, and spasmolytic properties. In Germany and Switzerland, metamizole is prescribed frequently because of its favorable gastrointestinal and renal tolerability compared to nonsteroidal anti-inflammatory drugs (NSAID), while exhibiting a similar analgesic and antipyretic activity (1-4). Metamizole is a prodrug, which, after oral application, is spontaneously hydrolyzed in the intestinal tract to N-methyl-4-aminoantipyrine (4-MAA) (5). 4-MAA is the major metabolite in plasma, which is demethylated to 4-aminoantipyrine (4-AA) or oxidized to 4-formylaminoantipyrine (4-FAA), an end metabolite. Furthermore, 4-AA is acetylated by N-acetyltransferase 2 (NAT2) to 4-acetylaminoantipyrine (4-AAA), another end metabolite (6-12). The metabolic pathway of metamizole is illustrated in Figure 1. The enzymes responsible for the demethylation and the oxidation of 4-MAA have so far not been conclusively identified. The prolonged half-life of 4-MAA in patients with impaired liver function suggests hepatic metabolism of 4-MAA with CYP3A4 as the most important CYP for N-demethylation (9, 12, 13). However, extrahepatic metabolism by myeloperoxidase in neutrophil granulocytes has also been described (14).

Several studies in humans have shown that metamizole can induce specific CYP enzymes. In liver microsomes extracted from biopsies of patients having been treated with metamizole, Saussele et al. showed that protein content and activity of CYP2B6 and CYP3A4 were increased compared to patients not treated with metamizole (15). Moreover, they showed that both 4-MAA and 4-AA increased the protein expression of CYP2B6 and CYP3A4 in primary human hepatocytes without directly interacting with the *constitutive androstane* (CAR) or the *pregnane X receptor* (PXR). Since these two nuclear receptors mediate induction of CYP2B6 and CYP3A4 along with other CYPs (16, 17), the mechanism of the metamizole derived CYP3A4 and CYP2B6 induction is currently unknown. Qin and colleagues confirmed CYP2B6 induction in healthy volunteers treated with 1.5 g metamizole per day for 4 days, as they observed a 2.1-fold increase in the bupropion hydroxylase activity after metamizole intake (18). Caraco et al. reported that the administration of metamizole decreased cyclosporine blood concentrations in patients after organ transplantation, suggesting CYP3A4 induction (19). Finally, Gaebler et al. found in a retrospective study that patients treated with metamizole had 67% lower sertraline plasma concentrations than patients without metamizole, suggesting CYP2B6 and CYP3A4 induction by metamizole (20). While the currently available studies suggest that metamizole is associated with CYP2B6 and possibly CYP3A4 induction, it remains unclear whether metamizole influences also other CYPs and which is the mechanism of CYP induction.

The interaction of a compound with CYPs can be investigated by a phenotyping cocktail approach, whereby specific substrates of CYPs are administered at subtherapeutic doses to quantify the metabolic activity of selected CYPs (21). The "*Basel phenotyping cocktail*", containing specific substrates for CYP1A2 (caffeine), CYP2B6 (efavirenz), CYP2C9 (flurbiprofen), CYP2C19 (omeprazole), CYP2D6 (metoprolol) and CYP3A4 (midazolam), has been proven to be a reliable tool to determine CYP inhibition as well as CYP induction (22-24). We therefore treated healthy subjects with metamizole and determined CYP activities before and after 7 days of metamizole ingestion (3 grams per day). Furthermore, we assessed the effect of 4-MAA on CYP induction and inhibition in wild type HepaRG cells and the interaction of 4-MAA with PXR and CAR using PXR or CAR knock-out HepaRG cells.

Material and Methods

Clinical Study

We conducted a single center, open-label phase I study (clinicaltrials.gov, ID: NCT03990129) with healthy male Caucasian volunteers. The study was approved by the ethics committee EKNZ (Ethikkommission Nordwestschweiz/Zentalschweiz) and conducted in accordance with good clinical practice guidelines and the current version of the Declaration of Helsinki.

Healthy male volunteers were screened for any underlying diseases (physical examination, routine laboratory, and electrocardiogram). The use of known enzyme inducers (e.g. St. John's Wort) or inhibitors (e.g. grapefruit juice) within 2 weeks before study start was an exclusion criterion as well as excessive caffeine consumption, smoking (>5 cigarettes per day) and use of over-the-counter medication.

After signing the informed consent, 12 healthy subjects were included (mean age: 25.0 years, range 21-28 years, mean body mass index: 22.9 kg/m^2, range 19.7-26.3 kg/m^2) into the study. A venous blood sample was drawn to determine routine laboratory parameters and the subjects' CYP2B6, CYP2C9, CYP2C19 and CYP2D6 genotype.

The subjects had to stop consuming caffeine containing nutrients 12 hours prior to both phenotyping cocktail administrations. For the baseline assessment of CYP activity, the subjects fasted overnight and arrived in the morning at the trial site. Prior to treatment, a blood sample was withdrawn from a venous catheter, placed in the non-dominant forearm, to determine the baseline drug concentrations of the subjects. Afterwards, the

"Basel phenotyping cocktail" capsule was administered containing 10 mg caffeine (CYP1A2 substrate), 2 mg midazolam (3A4 substrate), 50 mg efavirenz (CYP2B6 substrate), 12.5 mg flurbiprofen (CYP2C9 substrate), 10 mg omeprazole (CYP2C19 substrate), and 12.5 mg metoprolol tartrate (CYP2D6 substrate). Venous blood samples were withdrawn 0.25, 0.5, 0.75, 1, 2, 3, 4, 6, 8, 12 and 24 hours after cocktail administration into ethylenediaminetetraacetic acid (EDTA) coated tubes. Samples were centrifuged at 1500g for 10 minutes at 4°C and the plasma was stored at -80°C until analysis. On the second study day, the subjects began to take 3 times per day 1 g metamizole (2 Novalgin© 500 mg tablets) for 7 consecutive days. On study day 8, the subjects received in the morning for a second time the *"Basel phenotyping cocktail"* capsule, while metamizole administrations were continued until the afternoon to capture also potential CYP inhibition. The CYP phenotyping procedure was executed as on day 1.

To review compliance with metamizole treatment, subjects had to document their drug intake in a pill-counting journal and had to return the remaining tablets as well as the empty blisters. In addition, plasma levels of 4-MAA, 4-AA, 4-AAA and 4-FAA were monitored on study day 3 or 4 and 8 and compared to reference data (25).

In the middle of the study, routine hematology was assessed to exclude neutropenia, a rare and serious adverse reaction of metamizole (1, 26). Adverse events were documented throughout the entire study period.

Genotyping

Genotyping was performed as described before (27, 28). In addition, single nucleotide polymorphisms (SNPs) rs1057910 (CYP2C9*3, c.1075A>C, assay: C_27104892_10) and rs1799853 (CYP2C9*2, c.430C>T, assay: C_25625805_10) were determined, both associated with decreased CYP2C9 activity (29). The gene copy number was not assessed.

Study drugs

Capsules containing the "*Basel phenotyping cocktail*" were produced under GMP conditions by Dr. Hysek Apotheke, Biel, Switzerland as described before (24). Novalgin© was purchased through the University Hospital Pharmacy, Basel, Switzerland.

Chemicals and Reagents

Chemicals and reagents for the determination of the *"Basel phenotyping cocktail"* substrates and metabolites were purchased and prepared as described previously (30). Standards for the quantification of the metamizole metabolites were obtained and prepared as published before. Materials and reagents for the cell culture were ordered and used according to the protocols of a previous publication (14).

Bioanalysis

The analytes were quantified in plasma by high performance liquid chromatography (HPLC, Shimadzu, Kyoto, Japan) tandem mass spectrometry (ABSciex, Ontario, Canada). Analyses of the *"Basel phenotyping cocktail"* substrates and metabolites was conducted as described previously using an API 5500 Qtrap mass spectrometer (30). An API 4000 mass spectrometer was used to analyze the metabolites of metamizole according to a fully validated method (31). Data were processed using Analyst software 1.6.2 (ABSciex, Ontario, Canada).

Cell culture

All cells were grown at 37°C in a humidified 5% CO_2 cell culture incubator. HepaRG cells (Lot: 1964151) were purchased from Thermo Fisher Scientific (Wohlen, Switzerland). HepaRG cells were counted with the EVE® Automatic Cell counter and seeded at 300'000 cells per well into 6-well plates. They were cultured and differentiated as previously described (32). For induction assays, cells were treated for 72 hours with 300 µM 4-MAA, 10 µM rifampicin, 2 mM metformin or combinations of 4-MAA/metformin (300 µM/2 mM) and rifampicin/metformin (10 µM/2 mM). The vehicle concentration was 0.2% DMSO. During the induction assays, the medium containing the drugs was replaced every 24 hours.

hPXR-knockout HepaRG cells (Lot: 153429), hCAR-knockout HepaRG cells (Lot: 151345) and 5-F control HepaRG cells (Lot: 208137) were purchased from Sigma-Aldrich (Buchs, Switzerland). Culture and differentiation conditions were similar as described above, except that cell passaging required trypsin 0.25% (Thermo Fisher Scientific, Wohlen, Switzerland) instead of TrypLE® and the medium was changed trice instead of twice a week. After differentiation, all cells were incubated for 72 hours with 300 µM 4-MAA, or selective inducers (hPXR-knockout: 10 µM rifampicin, hCAR-knockout: 1 µM 6-(4-chlorophenyl)imidazo[2,1-b][1,3]thiazole-5-carbaldehyde O-(3,4-dichlorobenzyl)oxime (CITCO, Sigma-Aldrich, Buchs, Switzerland), 5-F control: 10 µM rifampicin and 1 µM CITCO). Fresh medium was replenished every 24 hours.

mRNA quantification

After induction, cells were harvested and mRNA was extracted and purified using Qiagen RNeasy Mini Extraction kit (Qiagen, Hilden, Germany). mRNA quantity and quality were determined with a NanoDrop 2000 UV-Vis spectrophotometer (Thermo Fisher Scientific, Wohlen, Switzerland). cDNA was synthesized with the Qiagen Omniscript system using 0.2-1 µg mRNA. Amplification reactions were performed in triplicate using SYBR green (Roche Diagnostics, Rotkreuz, Basel). Primers are listed in the suppl. Table 1. Real-time PCR was performed on a ViiA® 7 Real-Time PCR system (Applied Biosystems, Massachusetts, USA) and the relative quantity of specifically amplified cDNA was assessed using the comparative-threshold cycle method (33, 34). Glyceraldehyde 3-phosphate dehydrogenase (GAPDH) served as endogenous reference and no-template and no-reverse-transcription controls confirmed the absence of unspecific amplification.

Pharmacokinetic calculations and statistics

Primary endpoint of the study was the effect of metamizole treatment on the metabolic activity of CYP 1A2, 3A4, 2B6, 2C9, 2C19, and 2D6. CYP activity was determined by quantifying the following reactions: 1A2: caffeine to paraxanthine, 2B6: efavirenz to 8'-hydroxyefavirenz, 2C9: flurbiprofen to 4'-hydroxyflurbiprofen, 2C19: omeprazole to 5'-hydroxyomeprazole, 2D6: metoprolol to α-hydroxymetoprolol, 3A4: midazolam to 1'-hydroxymidazolam. The metabolic ratio (MR) was used as a measure for the individual CYP activity and calculated by dividing the area under the plasma concentration time curve (AUC_{inf}) of the probe drug by the AUC_{inf} of the corresponding metabolite. Caffeine and paraxanthine plasma concentrations were corrected because both were present in the baseline samples of every subject. The lowest concentration within the first two hours ($t_{0h\text{-}2h}$) post-dosing was set as the basal concentration C_0. We determined the individual elimination rate constant (k_e), calculated the residual concentration ($C_{residual}$) for every time point with the formula

$$C_{residual} = C_0 \times e^{-k_e \Delta t} \quad (1)$$

and subtracted the respective residual concentration from the measured concentration at each time point.

$AUC_{inf,}$ maximal plasma concentration (C_{max}), half-life ($t_{1/2}$) and elimination rate constant k_e of the cocktail drugs before and after treatment with metamizole were estimated with the non-compartmental methods using PKanalix (version 2019R1, Lixoft SAS, Abtony, France). AUCs were determined using the linear log trapezoidal method. The elimination rate constant was estimated using linear regression of log concentrations and time.

MR, $t_{1/2}$ and AUC_{inf} of the parent drugs were compared before and after metamizole treatment by the nonparametric Wilcoxon signed-rank test. *In vitro* conditions in different HepaRG cell systems were compared using one-way ANOVA with Dunnett's multiple comparison test. GraphPad Prism 8 (GraphPad Software, La Jolla, CA, US) was used for both analyses. A p value of <0.05 was considered as statistically significant (*: <0.05, **: <0.01, ***: <0.001, ****: <0.0001).

Results

Bioanalysis

As shown in the supplement, the analysis of the substrates and the metabolites of the *"Basel phenotyping cocktail"* as well as the metamizole metabolites met the criteria specified by the FDA guidelines for the bioanalysis of study samples (35).

Compliance

Inspection of the pill-counting journals and evaluation of the remaining tablets and the empty blisters suggested that all the subjects were compliant to the metamizole treatment regimen. Furthermore, as shown in suppl. Fig. 1, trough levels of the metamizole metabolites determined during and at the end of the study were detectable in all subjects. In comparison to a previous study with the same metamizole dosage in healthy subjects (25), the plasma concentration of all metabolites of the current were either above or within the trough concentration range of the previous study. Based on these results we assumed that the subjects were compliant to the metamizole treatment.

Effect of metamizole on plasma concentrations, AUC and MR of CYP substrates

The average plasma concentration-time curves of the 6 CYP probe drugs and their CYP-specific metabolites are shown in Fig. 2 and the corresponding pharmacokinetic parameters are listed in Table 1. The individual AUCs and the half-lives of the probe drugs are displayed in suppl. Fig. 2 and suppl. Fig. 3, respectively.

All subjects had residual caffeine and paraxanthine in their plasma, since they were allowed to consume caffeine-containing beverages up to 12 h before the study days 1 and 8. Therefore, the caffeine and

paraxanthine baseline levels were calculated using equation (1) and subtracted from the respective measured plasma concentrations to isolate the effect of 1A2 phenotyping. High caffeine and paraxanthine levels were observed in 24h samples of 3 subjects, indicating that these subjects had consumed caffeine between 12h and 24h post-treatment. These 24h values were excluded from the analysis and the corresponding 24h time-points were calculated using equation (1). Metamizole delayed the conversion of caffeine to paraxanthine, leading to a 1.79-fold increase in the caffeine AUC_{inf}, whereas the AUC_{inf} of paraxanthine was not significantly affected. In contrast to caffeine, metamizole decreased the elimination half-life for efavirenz and reduced the AUC_{inf} by 79%. The AUC_{inf} of 8´-hydroxyefavirenz, the principle metabolite formed by CYP2B6, was increased by 34%. Since 4'-hydroxyflurbiprofen, the principle metabolite of flurbiprofen formed by CYP2C9, can be glucuronidated (36), we determined 4'-hydroxyflurbiprofen after deglucuronidation. Metamizole decreased the elimination half-life and the AUC_{inf} of flurbiprofen by 22% and the AUC_{inf} of 4´-hydroxyflurbiprofen by 12%. Regarding omeprazole, the probe drug for CYP2C19, metamizole had no significant impact on the elimination velocity but decreased the AUC_{inf} by 66% and for 5´-hydroxyomeprazole by 32%. Metamizole did not significantly affect the elimination velocity of metoprolol, the probe drug for CYP2D6, but decreased the AUC_{inf} by 32% and of α-hydroxymetoprolol by 28%. The decrease in the AUC_{inf} of metoprolol and α-hydroxymetoprolol is most likely explained by the observation that CYP3A4, 2B6 and 2C9, which are induced by metamizole, contribute to O-demethylation and N-dealkylation of metoprolol (37). Metamizole decreased the elimination half-life of the CYP3A4 substrate midazolam and its AUC_{inf} by 68% and increased the AUC_{inf} of 1´-hydroxymidazolam (determined after deglucuronidation) by 22%.

The individual metabolic ratios are displayed in Fig 3. For CYP1A2, we found a significant increase in the caffeine:paraxanthine MR with metamizole, indicating inhibition (p=0.0024). We found a reduction in the efavirenz:8'-hydroxyefavirenz MR from 90.4 to 13.9, demonstrating CYP2B6 induction by metamizole (p=0.0005). Similarly, metamizole lowered the flurbiprofen:4'-hydroxyflurbiprofen MR (from 13.8 to 12.2), indicating CYP2C9 induction (p=0.0342). Furthermore, metamizole reduced the MR of omeprazole to 5'-hydroxyomeprazole by approximately 50% (p=0.0005), demonstrating CYP2C19 induction. CYP2D6 is described in the literature as not inducible (22). In agreement with this notion, we observed no significant change in the MR of metoprolol by metamizole. In contrast, CYP3A4 activity was induced by metamizole as demonstrated by the decrease in the midazolam:1'-hydroxymidazolam MR from 0.40 to 0.10 (p=0.0005).

Genotype, inducibility and phenotype correlation

All subjects were analyzed for the SNPs CYP1A2*1F; CYP2B6 *6; CYP2C9*2, *3; CYP2C19*2, *17; CYP2D6*2, *3, *4, *6, *9,*10, *17, *29, and *41 in order to identify poor (PM), intermediate (IM), normal (NM), rapid (RM) and ultra-rapid metabolizers (UM) for the respective CYPs and to investigate their influence on the phenotyping results. The individual values are displayed in suppl. Table 2.

To judge a possible effect of the genotype on inducibility, we calculated the ratio of $MR_{-Metamizole}$:$MR_{+Metamizole}$ and correlated the values with the genotype of the subjects (Figure 4). The relationship between genotype and the basal MR is shown in suppl. Fig. 4. Five subjects were homozygous for CYP1A2*1F (classified as NM/UM), a genotype associated with higher inducibility of CYP1A2, for instance in smokers (38). Since we did not include heavy smokers, we did not expect an impact of *1F genotype on the MR of caffeine. The data illustrated in suppl. Fig. 4 confirmed this assumption. Carriers of the CYP1A2*1F genotype showed a similar distribution of the $MR_{-Metamizole}$:$MR_{+Metamizole}$ ratio as wild types (Fig. 4), indicating that the *1F genotype did not affect CYP1A2 inhibition by metamizole. CYP2B6*6 is associated with impaired efavirenz metabolism (39). The population studied included 8 heterozygous (*1/*6) and 4 wild-type allele carriers (*1/*1), categorized as IM and NM, respectively. Considering the genotype-phenotype correlation in the basal state, the MR of NM and IM were similar (96.3 vs. 87.5 in NM vs. IM) (suppl. Fig. 4). As shown in Fig. 4, the $MR_{-Metamizole}$:$MR_{+Metamizole}$ of NM and IM were comparable, indicating that the *6 genotype did not affect the inducibility of CYP2B6. Regarding CYP2C9, we found 5 NM (*1/*1), 3 heterozygous CYP2C9*2 carriers (*1/*2) and 3 heterozygous CYP2C9*3 carriers (*1/*3), both categorized as IM, and one homozygous CYP2C9*3 carrier, categorized as PM (29). Surprisingly, the subject with the highest MR was an NM and not, as expected, the only PM. The only PM among the subjects had unexpectedly one of the lowest MR (suppl. Fig. 4), suggesting the presence of additional SNPs affecting the phenotype. As shown in Fig. 4, the $MR_{-Metamizole}$:$MR_{+Metamizole}$ ratios among NM, IM and PM were not different, suggesting that the genotype did not affect the inducibility of CYP2C9. Genotyping of CYP2C19 revealed 7 NM (*1/*1), 2 heterozygous carriers of the CYP2C19*2 allele (*1/*2 and *2/*17) classified as IM and 3 heterozygous carriers of the CYP2C19 *1/*17 variant classified as RM (40). Although not statistically significant due to the small number of subjects, we would not exclude the possibility that IM have impaired CYP2C19 inducibility (Fig. 4). Regarding the effect on the basal MR, CYP2C19 IM had the highest and RM the lowest values but this difference did not reach statistical significance due to the small number of subjects investigated (suppl. Fig. 4). Concerning CYP2D6, we found 9 NM (*1/*1, *1/*2, *2/*2, *1/*41 or *2/*41 diplotype, activity score 1.25-2.25) and 3 IM (*4/*10 or *29/41 diplotype, activity score

0.25-1.00). The SNPs *10, *29 and *41 are associated with decreased CYP2D6 activity, and the *4 allele with no activity (41-43). As shown in Fig. 4, the inducibility appeared not to be affected by metamizole.

Mechanism of CYP induction

We used differentiated HepaRG cells, which have a hepatocyte-like morphology and a similar expression and activity of most CYPs as human hepatocytes (32). As shown in Fig. 5, treatment with 300 µM 4-MAA for 72 hours increased the mRNA content of CYP2B6, CYP2C9, CYP2C19 and CYP3A4 significantly (4.8-fold, 1.4-fold, 1.5-fold and 2.0-fold, respectively), while CYP1A2 and CYP2D6 were unaffected. Incubation with 10 µM rifampicin, a PXR activator (44), resulted in an increased mRNA content of the same CYPs (CYP2B6 4.3-fold, CYP2C9 1.4-fold, CYP2C19 2.2-fold, CYP3A4 6.0-fold), proving the functionality of the system. Co-incubation with metformin, an inhibitor of PXR and CAR mediated CYP induction (45), suppressed both 4-MAA and rifampicin induced upregulation of CYP mRNAs. CYP2D6 mRNA expression was not significantly affected, whereas metformin suppressed also CYP1A2 mRNA expression, suggesting a negative effect on the aryl hydrocarbon receptor (46).

To further investigate the role of both CAR and PXR in 4-MAA mediated CYP induction, CAR-knockout, PXR-knockout, and control HepaRG cells (5-F cells) were treated for 72 hours with 300 µM 4-MAA and specific ligands for the respective nuclear receptors (CAR: 1 µM CITCO, PXR: 10 µM rifampicin) (Fig. 6). In 5-F cells (corresponding to HepaRG wild type cells), 4-MAA showed the expected induction of the mRNA of CYP2B6, 2C9, 2C19 and 3A4. Surprisingly, CITCO not only induced the mRNA of CYP2B6 and 2C19 (the increases in CYP3A4 and 2C9 mRNA were not significant), but also of CYP1A2. Rifampicin increased the mRNA expression of CYP2C19 and 3A4, whereas the increases in the mRNA of CYP2B6 and 2C9 were not significant. In HepaRG cells lacking CAR, 4-MAA exhibited only a minor CYP2C9 mRNA induction, whereas CITCO still induced CYP1A2, but no other CYPs. In HepaRG cells lacking PXR, 4-MAA induced mRNA expression of CYP2B6, 2C9, 2C19 and CYP3A4, whereas rifampicin showed no CYP induction. The results indicate that CAR expression is essential for CYP mRNA induction by 4-MAA.

Discussion

Metamizole has been used as an analgesic drug for nearly a century in multiple regions of the world. So far, the potential that metamizole can induce CYP2B6 and CYP3A4 has been suggested in one *in vitro* investigation (15) and in 3 clinical studies (18-20). In one of these studies, Qin et al. found a significantly increased

bupropion hydroxylation after four days of metamizole treatment in 16 healthy males (18), suggesting that metamizole induces CYP2B6 activity. The authors suspected CYP2B6 induction via an interaction with CAR because of the structural similarity of metamizole with phenobarbital and the concomitantly increased hydroxybupropion clearance. Metabolism of hydroxybupropion is UDP-glucuronosyltransferase dependent, whose induction depends on CAR (47). Some years earlier, Saussele et al. had observed increased expression and activity of CYP2B6 and CYP3A4 in human liver microsomes from patients treated with metamizole and confirmed induction of CYP2B6 and CYP3A4 by 4-MAA in primary human hepatocytes but reporter-gene assays failed to show a direct PXR or CAR activation by 4-MAA (15). Similar to Qin et al., they also suspected a phenobarbital-like mechanism of induction due the structural similarity of metamizole and phenobarbital (15). Although phenobarbital is known to induce various CYPs via indirect activation of CAR (48), it has been shown recently that CYP3A4 induction by phenobarbital is mainly mediated via PXR (49). In support of the notion that metamizole can induce CYP2B6 and CYP3A4, Gaebler et al. reported decreased sertraline serum concentrations (20) and Caraco et al. decreased cyclosporine blood concentrations in patients treated concomitantly with metamizole (19). Taken together, there was some evidence that metamizole induces CYP2B6 and CYP3A4 whereas information about induction of other CYPs and the mechanism of CYP induction was lacking. We therefore conducted a single center crossover study to assess the effect of metamizole treatment on 6 specific CYP substrates (CYP1A2, CYP2B6, CYP2C9, CYP2C19, CYP2D6 and CYP3A4) using the cocktail approach.

We observed a significant decrease in the metabolic ratios for efavirenz, flurbiprofen, omeprazole and midazolam, demonstrating a moderate induction of CYP2B6, 2C19 and 3A4 and a weak induction of CYP2C9. While CYP2B6 and CYP3A4 upregulation due to metamizole are in line with the previously published studies (15, 18, 19, 50), induction of CYP2C9 and CYP2C19 has so far not been reported. Surprisingly, we found a decreased metabolism of caffeine to paraxanthine by metamizole, indicating weak inhibition of CYP1A2. Since there is some evidence that CYP1A2 may be involved in the demethylation of 4-MAA (51), it is possible that the observed decrease in CYP1A2 activity is the result of a competition between 4-MAA and caffeine.

We could not detect an impact of the genotype on the inducibility of CYP2B6, CYP2C9 and CYP2C19. However, these findings must be viewed with caution considering the limited number of subjects studied. Furthermore, with our genetic analysis we only assessed single nucleotide polymorphisms, but not the number of gene copies. Thus, we could have missed CYP2D6 ultra-rapid metabolizers. Considering that we found no induction

of CYP2D6, it is, however, unlikely that this omission has an impact on the interpretation of the results of this study.

To confirm the results of the clinical study, we performed *in vitro* experiments in HepaRG cells. After differentiation, this human hepatoma cell line has similar drug metabolizing properties as human hepatocytes (32). After 72 hours of treatment with 300 µM 4-MAA, we observed a significant increase in CYP2B6, CYP2C9, CYP2C19 and CYP3A4 mRNA, which confirmed the findings of our clinical study. Incubation of HepaRG cells with rifampicin showed upregulation of CYP2B6, CYP2C9, CYP2C19 and CYP3A4 as shown previously (32), proving the validity of the chosen *in vitro* model. Co-incubation with metformin, an inhibitor of CAR and PXR (52), blocked both 4-MAA and rifampicin-mediated induction. Since activation of CAR and PXR is associated with upregulation of CYP2B, CYP2C and CYP3A, it was at this point not clear via which transcription factor MAA acted as a CYP inducer (47).

To answer this question, we treated HepaRG cells carrying a stable PXR or CAR knock-out and corresponding 5-F control HepaRG cells with 4-MAA and selective inducers (CITCO for CAR and rifampicin for PXR) to verify the functionality of the knock-out. In 5-F control cells, we observed the expected induction of CYP2B6, CYP2C9, CYP2C19 and CYP3A4 mRNA by MAA and to a variable extent also by CITCO and rifampicin. To our surprise, CITCO also induced CYP1A2 in CAR knock-out and 5-F control cells, suggesting an interaction with the aryl hydrocarbon receptor. This phenomenon has been described in similar experiments before (53). While PXR knock-out HepaRG cells showed a comparable upregulation of CYP2C9 and CYP2C19 mRNA and an even more extensive induction of CYP2B6 and CYP3A4 mRNA compared to the 5-F control cell line in the presence of 4-MAA, CAR knock-out HepaRG did not show a significant upregulation by 4-MAA, except for CYP2C9. The specific inducers CITCO and rifampicin showed no CYP mRNA induction in the absence of the nuclear factor that they activate. These results show that 4-MAA-derived induction of CYP2B6, 2C9, 2C19 and 3A4 is mediated via CAR activation. Our study does not answer the question, however, whether the induction via CAR is direct or indirect.

In conclusion, metamizole is a broad CYP inducer via its major metabolite 4-MAA, which interacts directly or indirectly with CAR. In addition, metamizole is an inhibitor of CYP1A2. Regarding the widespread use of this analgesic in some countries, particularly in the elderly with numerous comedications, these interactions are of major clinical relevance.

Author contributions

F.B., U.D. and S.K. wrote the manuscript; F.B. and S.K. designed the research; F.B., U.D. M.P. and H.M. performed the research; F.B., U.D. and S.K. analyzed the data; H.M., U.D., M.H., M.P. and J.H. contributed analytical tools and the phenotyping tools; M.H. critically commented the manuscript.

Acknowledgements

We would like to thank our study nurses Claudia Bläsi and Joyce Jesus de Santos for their valuable help in study preparation and conduction.

Study Highlights

What is the current knowledge on the topic?

Several studies indicate that metamizole is an inducer of CYP2B6 and CYP3A4. However, no studies have so far been conducted to elucidate the interaction potential of metamizole for other CYPs. Furthermore, the mechanism of induction is currently not known.

What question did this study address?

This study addressed the influence of metamizole on the activity of CYP1A2, CYP2B6, CYP2C9, CYP2C19 and CYP3A4 in healthy volunteers. Additionally, *in vitro* experiments were conducted to explore the mechanism of CYP induction.

What does the study add to our knowledge?

The results of the clinical study show that metamizole weakly inhibits the activity of CYP1A2 and moderately induces CYP2B6, CYP2C19 and CYP3A4 and weakly induces CYP2C9. Interaction with the *constitutive androstane receptor* is needed for the induction for CYP induction.

How might this change clinical pharmacology and translational science?

This study adds valuable information about the drug-drug interaction potential of metamizole. Since metamizole is often used also in the geriatric population with a high prevalence of polypharmacy, this information is clinically important.

References

(1) Blaser, L.S., Tramonti, A., Egger, P., Haschke, M., Krähenbühl, S. & Rätz Bravo, A.E. Hematological safety of metamizole: retrospective analysis of WHO and Swiss spontaneous safety reports. *European Journal of Clinical Pharmacology* **71**, 209-17 (2015).

(2) Hoffmann, F., Meinecke, P., Freitag, M.H., Glaeske, G., Schulze, J. & Schmiemann, G. Who gets dipyrone (metamizole) in Germany? Prescribing by age, sex and region. *Journal of Clinical Pharmacy and Therapeutics* **40**, 285-8 (2015).

(3) Andrade, S.E., Martinez, C. & Walker, A.M. Comparative Safety Evaluation of Non-narcotic Analgesics. *Journal of Clinical Epidemiology* **51**, 1357-65 (1998).

(4) Sánchez, S., De La Lastra, C.A., Ortiz, P., Motilva, V. & Martín, M.J. Gastrointestinal Tolerability of Metamizol, Acetaminophen, and Diclofenac in Subchronic Treatment in Rats. *Digestive Diseases and Sciences* **47**, 2791-8 (2002).

(5) Ergün, H., Frattarelli, D.A.C. & Aranda, J.V. Characterization of the role of physicochemical factors on the hydrolysis of dipyrone. *Journal of Pharmaceutical and Biomedical Analysis* **35**, 479-87 (2004).

(6) Noda, A., Goromaru, T., Tsubone, N., Matsuyama, K. & Iguchi, S. In vivo formation of 4-formylaminoantipyrine as a new metabolite of aminopyrine. I. *Chem Pharm Bull (Tokyo)* **24**, 1502-5 (1976).

(7) Noda, A., Tsubone, N., Mihara, M., Goromaru, T. & Iguchi, S. Formation of 4-formylaminoantipyrine as a new metabolite of aminopyrine. II. Enzymatic demethylation and oxidation of aminopyrine and 4-monomethylaminoantipyrine. *Chem Pharm Bull (Tokyo)* **24**, 3229-31 (1976).

(8) Volz, M. & Kellner, H.M. Kinetics and metabolism of pyrazolones (propyphenazone, aminopyrine and dipyrone). *Br J Clin Pharmacol* **10 Suppl 2**, 299S-308S (1980).

(9) Levy Micha, Z.-K.E., Rosenkranz Bernd. Clinical Pharmacokinetics of Dipyrone and its Metabolites. *Clinical Pharmacokinetics* **28**, 216-34 (1995).

(10) Zylber-Katz, E., Granit, L. & Levy, M. Formation and excretion of dipyrone metabolites in man. *Eur J Clin Pharmacol* **42**, 187-91 (1992).

(11) Flusser, D., Zylber-Katz, E., Granit, L. & Levy, M. Influence of food on the pharmacokinetics of dipyrone. *Eur J Clin Pharmacol* **34**, 105-7 (1988).

(12) Agundez, J.A., Martinez, C. & Benitez, J. Metabolism of aminopyrine and derivatives in man: in vivo study of monomorphic and polymorphic metabolic pathways. *Xenobiotica* **25**, 417-27 (1995).

(13) Geisslinger, G., Bocker, R. & Levy, M. High-performance liquid chromatographic analysis of dipyrone metabolites to study their formation in human liver microsomes. *Pharm Res* **13**, 1272-5 (1996).

(14) Bachmann, F., Duthaler, U., Rudin, D., Krahenbuhl, S. & Haschke, M. N-demethylation of N-methyl-4-aminoantipyrine, the main metabolite of metamizole. *Eur J Pharm Sci* **120**, 172-80 (2018).

(15) Saussele, T. *et al.* Selective induction of human hepatic cytochromes P450 2B6 and 3A4 by metamizole. *Clin Pharmacol Ther* **82**, 265-74 (2007).

(16) Pelkonen, O., Turpeinen, M., Hakkola, J., Honkakoski, P., Hukkanen, J. & Raunio, H. Inhibition and induction of human cytochrome P450 enzymes: current status. *Arch Toxicol* **82**, 667-715 (2008).

(17) Hewitt, N.J., Lecluyse, E.L. & Ferguson, S.S. Induction of hepatic cytochrome P450 enzymes: methods, mechanisms, recommendations, and in vitro-in vivo correlations. *Xenobiotica* **37**, 1196-224 (2007).

(18) Qin, W.J. *et al.* Rapid clinical induction of bupropion hydroxylation by metamizole in healthy Chinese men. *Br J Clin Pharmacol* **74**, 999-1004 (2012).

(19) Caraco, Y., Zylber-Katz, E., Fridlander, M., Admon, D. & Levy, M. The effect of short-term dipyrone administration on cyclosporin pharmacokinetics. *Eur J Clin Pharmacol* **55**, 475-8 (1999).

(20) Gaebler, A.J. *et al.* Metamizole but not ibuprofen reduces the plasma concentration of sertraline: Implications for the concurrent treatment of pain and depression/anxiety disorders. *Br J Clin Pharmacol*, (2020).

(21) Zhou, H., Tong, Z. & McLeod, J.F. "Cocktail" approaches and strategies in drug development: valuable tool or flawed science? *J Clin Pharmacol* **44**, 120-34 (2004).

(22) Derungs, A., Donzelli, M., Berger, B., Noppen, C., Krahenbuhl, S. & Haschke, M. Effects of Cytochrome P450 Inhibition and Induction on the Phenotyping Metrics of the Basel Cocktail: A Randomized Crossover Study. *Clin Pharmacokinet* **55**, 79-91 (2016).

(23) Donzelli, M. *et al.* The basel cocktail for simultaneous phenotyping of human cytochrome P450 isoforms in plasma, saliva and dried blood spots. *Clin Pharmacokinet* **53**, 271-82 (2014).

(24) Camblin, M., Berger, B., Haschke, M., Krahenbuhl, S., Huwyler, J. & Puchkov, M. CombiCap: A novel drug formulation for the basel phenotyping cocktail. *Int J Pharm* **512**, 253-61 (2016).

(25) Blaser, L. *et al.* Effect of metamizole (dipyrone) on renal function in salt-depleted healthy subjects. (Submitted, 2020).

(26) Blaser, L. *et al.* Leucopenia associated with metamizole: a case-control study. *Swiss medical weekly* **147**, w14438 (2017).

(27) Vizeli, P., Schmid, Y., Prestin, K., Meyer Zu Schwabedissen, H.E. & Liechti, M.E. Pharmacogenetics of ecstasy: CYP1A2, CYP2C19, and CYP2B6 polymorphisms moderate pharmacokinetics of MDMA in healthy subjects. *Eur Neuropsychopharmacol* **27**, 232-8 (2017).

(28) Schmid, Y., Vizeli, P., Hysek, C.M., Prestin, K., Meyer Zu Schwabedissen, H.E. & Liechti, M.E. CYP2D6 function moderates the pharmacokinetics and pharmacodynamics of 3,4-methylene-dioxymethamphetamine in a controlled study in healthy individuals. *Pharmacogenet Genomics* **26**, 397-401 (2016).

(29) Van Booven, D. *et al.* Cytochrome P450 2C9-CYP2C9. *Pharmacogenetics and Genomics* **20**, 277-81 (2010).

(30) Suenderhauf, C. *et al.* Pharmacokinetics and phenotyping properties of the Basel phenotyping cocktail combination capsule in healthy male adults. *Br J Clin Pharmacol* **86**, 352-61 (2020).

(31) Bachmann, F., Blaser, L., Haschke, M., Krahenbuhl, S. & Duthaler, U. Development and validation of an LC-MS/MS method for the bioanalysis of the major metamizole metabolites in human plasma. *Bioanalysis* **12**, 175-89 (2020).

(32) Berger, B. *et al.* Comparison of Liver Cell Models Using the Basel Phenotyping Cocktail. *Front Pharmacol* **7**, 443 (2016).

(33) Grunig, D., Felser, A., Bouitbir, J. & Krahenbuhl, S. The catechol-O-methyltransferase inhibitors tolcapone and entacapone uncouple and inhibit the mitochondrial respiratory chain in HepaRG cells. *Toxicol In Vitro* **42**, 337-47 (2017).

(34) Guillouzo, A., Corlu, A., Aninat, C., Glaise, D., Morel, F. & Guguen-Guillouzo, C. The human hepatoma HepaRG cells: a highly differentiated model for studies of liver metabolism and toxicity of xenobiotics. *Chem Biol Interact* **168**, 66-73 (2007).

(35) Quiros, P.M., Goyal, A., Jha, P. & Auwerx, J. Analysis of mtDNA/nDNA Ratio in Mice. *Current protocols in mouse biology* **7**, 47-54 (2017).

(36) Spraul, M., Hofmann, M., Wilson, I.D., Lenz, E., Nicholson, J.K. & Lindon, J.C. Coupling of HPLC with 19F- and 1H-NMR spectroscopy to investigate the human urinary excretion of flurbiprofen metabolites. *J Pharm Biomed Anal* **11**, 1009-15 (1993).

(37) Berger, B., Bachmann, F., Duthaler, U., Krahenbuhl, S. & Haschke, M. Cytochrome P450 Enzymes Involved in Metoprolol Metabolism and Use of Metoprolol as a CYP2D6 Phenotyping Probe Drug. *Front Pharmacol* **9**, 774 (2018).

(38) Wang, L., Hu, Z., Deng, X., Wang, Y., Zhang, Z. & Cheng, Z.N. Association between common CYP1A2 polymorphisms and theophylline metabolism in non-smoking healthy volunteers. *Basic Clin Pharmacol Toxicol* **112**, 257-63 (2013).

(39) Nyakutira, C. *et al.* High prevalence of the CYP2B6 516G-->T(*6) variant and effect on the population pharmacokinetics of efavirenz in HIV/AIDS outpatients in Zimbabwe. *Eur J Clin Pharmacol* **64**, 357-65 (2008).

(40) Santos, P.C. *et al.* CYP2C19 and ABCB1 gene polymorphisms are differently distributed according to ethnicity in the Brazilian general population. *BMC Med Genet* **12**, 13 (2011).

(41) Crews, K.R. *et al.* Clinical Pharmacogenetics Implementation Consortium (CPIC) guidelines for codeine therapy in the context of cytochrome P450 2D6 (CYP2D6) genotype. *Clin Pharmacol Ther* **91**, 321-6 (2012).

(42) Hicks, J.K. *et al.* Clinical Pharmacogenetics Implementation Consortium (CPIC) Guideline for CYP2D6 and CYP2C19 Genotypes and Dosing of Selective Serotonin Reuptake Inhibitors. *Clin Pharmacol Ther* **98**, 127-34 (2015).

(43) Hicks, J.K. *et al.* Clinical Pharmacogenetics Implementation Consortium guideline for CYP2D6 and CYP2C19 genotypes and dosing of tricyclic antidepressants. *Clin Pharmacol Ther* **93**, 402-8 (2013).

(44) Fuhr, U. Induction of drug metabolising enzymes: pharmacokinetic and toxicological consequences in humans. *Clin Pharmacokinet* **38**, 493-504 (2000).

(45) Krausova, L. *et al.* Metformin suppresses pregnane X receptor (PXR)-regulated transactivation of CYP3A4 gene. *Biochem Pharmacol* **82**, 1771-80 (2011).

(46) Nebert, D.W., Dalton, T.P., Okey, A.B. & Gonzalez, F.J. Role of aryl hydrocarbon receptor-mediated induction of the CYP1 enzymes in environmental toxicity and cancer. *J Biol Chem* **279**, 23847-50 (2004).

(47) Tolson, A.H. & Wang, H. Regulation of drug-metabolizing enzymes by xenobiotic receptors: PXR and CAR. *Adv Drug Deliv Rev* **62**, 1238-49 (2010).

(48) Corcos, L. & Lagadic-Gossmann, D. Gene induction by Phenobarbital: an update on an old question that receives key novel answers. *Pharmacol Toxicol* **89**, 113-22 (2001).

(49) Li, L. *et al.* Mechanistic Insights of Phenobarbital-Mediated Activation of Human but Not Mouse Pregnane X Receptor. *Mol Pharmacol* **96**, 345-54 (2019).

(50) Kraul, H. *et al.* Immunohistochemical properties of dipyrone-induced cytochromes P450 in rats. *Hum Exp Toxicol* **15**, 45-50 (1996).

(51) Blanco, G., Martínez, C., García-Martín, E. & Agúndez, J.A.G. Cytochrome P450 Gene Polymorphisms and Variability in Response to NSAIDs. *Clinical Research and Regulatory Affairs* **22**, 57-81 (2005).

(52) Chai, S.C., Cherian, M.T., Wang, Y.M. & Chen, T. Small-molecule modulators of PXR and CAR. *Biochim Biophys Acta* **1859**, 1141-54 (2016).

(53) Li, D. *et al.* Genome-wide analysis of human constitutive androstane receptor (CAR) transcriptome in wild-type and CAR-knockout HepaRG cells. *Biochem Pharmacol* **98**, 190-202 (2015).

Figure legends

Figure 1

Scheme of the metabolic pathway of metamizole. Metamizole is non-enzymatically hydrolyzed in the gastrointestinal tract to N-methyl-4-aminoantipyrine (4-MAA), which has a high bioavailability. Later on, 4-MAA is enzymatically oxidized to N-formyl-4-aminoantipyrine (4-FAA) or demethylated to 4-aminoantipyrine (4-AA). 4-AA can be further acetylated by N-acetyltransferase 2 to N-acetyl-4-aminoantipyrine (4-AAA).

Figure 2

Plasma concentration-time profiles of the constituents of the "Basel phenotyping cocktail" substrates and their CYP-specific metabolite before and at the end of treatment with metamizole. Healthy subjects (n = 12) were treated with a capsule of the *"Basel phenotyping cocktail"* containing caffeine, efavirenz, flurbiprofen, omeprazole, metoprolol and midazolam before (white circle) and after intake of 3 times per day 1 g metamizole for 7 consecutive days (black circle). Plasma concentrations were determined by LC-MS/MS. Plasma concentrations for caffeine and paraxanthine were baseline corrected. Data are presented as mean ± SEM.

Figure 3

Metabolic ratios of the six substrates contained in the "Basel phenotyping cocktail" before and at the end of treatment with metamizole. Healthy subjects (n = 12) were treated with a capsule of the "*Basel phenotyping cocktail*" containing caffeine (**1A2**), efavirenz (**2B6**), flurbiprofen (**2C9**), omeprazole (**2C19**), metoprolol (**2D6**) and midazolam (**3A4**) before and at the end of treatment with metamizole (3 x 1 g per day for 7 days). Plasma concentrations were determined using LC-MS/MS. Metabolic ratios were calculated as the AUC_{inf} of the parent drug divided by the AUC_{inf} of the CYP-specific metabolite. Data represent individual values before (-Metamizole, white circles) and after (+Metamizole, black circles) treatment with metamizole. The black line corresponds to the geometric mean. *p<0.05, **p<0.01 and ***p<0.001 vs. values before treatment with metamizole (baseline).

Figure 4

Effect of the CYP genotype on CYP inducibility and inhibition. Genotyping of CYP1A2, CYP2B6, CYP2C9, CYP2C19, and CYP2D6 was performed for all 12 healthy subjects by real time PCR. For CYP3A4, no genotyping

was performed. The genotypes are presented on the x-axis. For phenotyping, the same subjects received the "*Basel phenotyping cocktail*" capsule containing caffeine (**1A2**), efavirenz (**2B6**), flurbiprofen (**2C9**), omeprazole (**2C19**), metoprolol (**2D6**) and midazolam (**3A4**) before and at the end of treatment with metamizole (3 x 1 g per day for 7 days). Metabolic ratios (MR) were calculated as the AUC_{inf} of the parent drug divided by the AUC_{inf} of the CYP-specific metabolite. CYP inducibility was assessed as the ratio of the MRs before and at the end of treatment with metamizole. The $MR_{-Metamizole}$:$MR_{+Metamizole}$ ratios are presented according to the genotype (PM: poor metabolizer, IM: intermediate metabolizer, NM: normal metabolizer, RM: rapid metabolizer, UM: ultrarapid metabolizer). The boxes represent the 25th to 75th percentile and the line in the middle corresponds to the median value. The whiskers designate the range of the data. The statistical analysis using t-tests or Mann-Whitney tests (CYP1A2, 2B6, 2C9 and 2D6) or a one-way ANOVA (2C19) revealed no significant effect of the genotype on the corresponding $MR_{-Metamizole}$:$MR_{+Metamizole}$ ratio.

Figure 5

Induction of different CYPs mRNA expression in differentiated HepaRG cells by N-methyl-4-aminoantipyrine (4-MAA). After differentiation, cells were treated with 300 µM 4-MAA for 72 h. Treatment with 10 µM rifampicin was used as a positive control. The PXR and CAR inhibitor metformin was used at a concentration of 2 mM. Data are presented as the mean ± SEM. *p<0.05, **p<0.01, ***p<0.001 and ****p<0.0001 vs. DMSO control incubations.

Figure 6

Induction of different CYPs mRNA expression in HepaRG cells with stable knock-out of CAR (-/- CAR) or PXR (-/- PXR) and control cells (5-F) by N-methyl-4-aminoantipyrine (4-MAA). After differentiation, cells were treated with 300 µM 4-MAA for 72 h. Treatment with 10 µ rifampicin was used as a positive control for PXR stimulation and 1 µM CITCO for CAR stimulation. Data are presented as the mean ± SEM. *p<0.05, **p<0.01, ***p<0.001 and ****p<0.0001 vs. the respective DMSO control incubations.

Table 1. *Effect of metamizole on the pharmacokinetics and the metabolic ratios of the substrates contained in the "Basel phenotyping cocktail".* 12 healthy subjects were treated with a capsule of the "*Basel phenotyping cocktail*" containing caffeine, efavirenz, flurbiprofen, omeprazole, metoprolol and midazolam before and at the end of treatment with metamizole (3 x 1 g per day for 7 days). AUC: area under the curve, $t_{1/2}$: half-life. Numbers represent the geometric mean, while the 95% confidence interval of the geometric mean is represented in brackets. *p<0.05, **p<0.01 and ***p<0.001 vs. values before treatment with metamizole (basal).

	basal	post treatment	basal	post treatment	basal	post treatment
	AUC_{inf} [µg x h/L]	AUC_{inf} [µg x h/L]	metabolic ratio	metabolic ratio	$t_{1/2}$ [h]	$t_{1/2}$ [h]
Caffeine	7211 (5793-8977)	12912** (8001-20836)	1.54 (1.21-1.97)	2.80** (1.77-4.42)	5.02 (4.21-6.00)	8.60* (5.48-13.5)
Paraxanthine	4676 (3817-5728)	4618 (3113-6853)				
Efavirenz	3978 (2926-5408)	821*** (591-1411)	90.4 (53.3-153)	13.9***(9.65-19.0)	37.8 (24.6-58.0)	15.2** (10.4-22.3)
8'-hydroxyefavirenz	44.0 (31.5-61.6)	59.3 (40.3-87.2)				
Flurbiprofen	10015 (7751-12941)	7779*** (5847-10350)	13.8 (8.71-21.9)	12.2* (7.40-20.3)	6.35 (5.08-7.94)	5.21*** (3.92-6.91)
4'-hydroxyflurbiprofen	726 (561-939)	636** (487-830)				
Omeprazole	187 (138-253)	62.9*** (45.4-86.9)	0.84 (0.63-1.12)	0.42*** (0.30-0.57)	0.74 (0.63-0.86)	0.75 (0.66-0.85)
5'-hydroxyomeprazole	222 (197-252)	152*** (127-181)				
Metoprolol	41.4 (28.0-61.2)	28.3* (17.1-46.8)	0.57 (0.37-0.91)	0.55 (0.33-1.91)	3.64 (3.10-4.26)	3.40 (2.76-4.15)
α-hydroxymetoprolol	72.0 (62.4-83.0)	51.7** (46.1-58.0)				

Midazolam	19.7 (14.6-26.7)	6.25** (3.54-11.0)	0.40 (0.28-0.57)	0.10*** (0.06-0.19)	2.44 (2.03-2.94)	1.60** (1.23-2.06)
1'-hydroxymidazolam	49.0 (41.3-58.0)	59.7* (50.4-70.6)				

Supplemental Files

1. Supplemental Material.docx

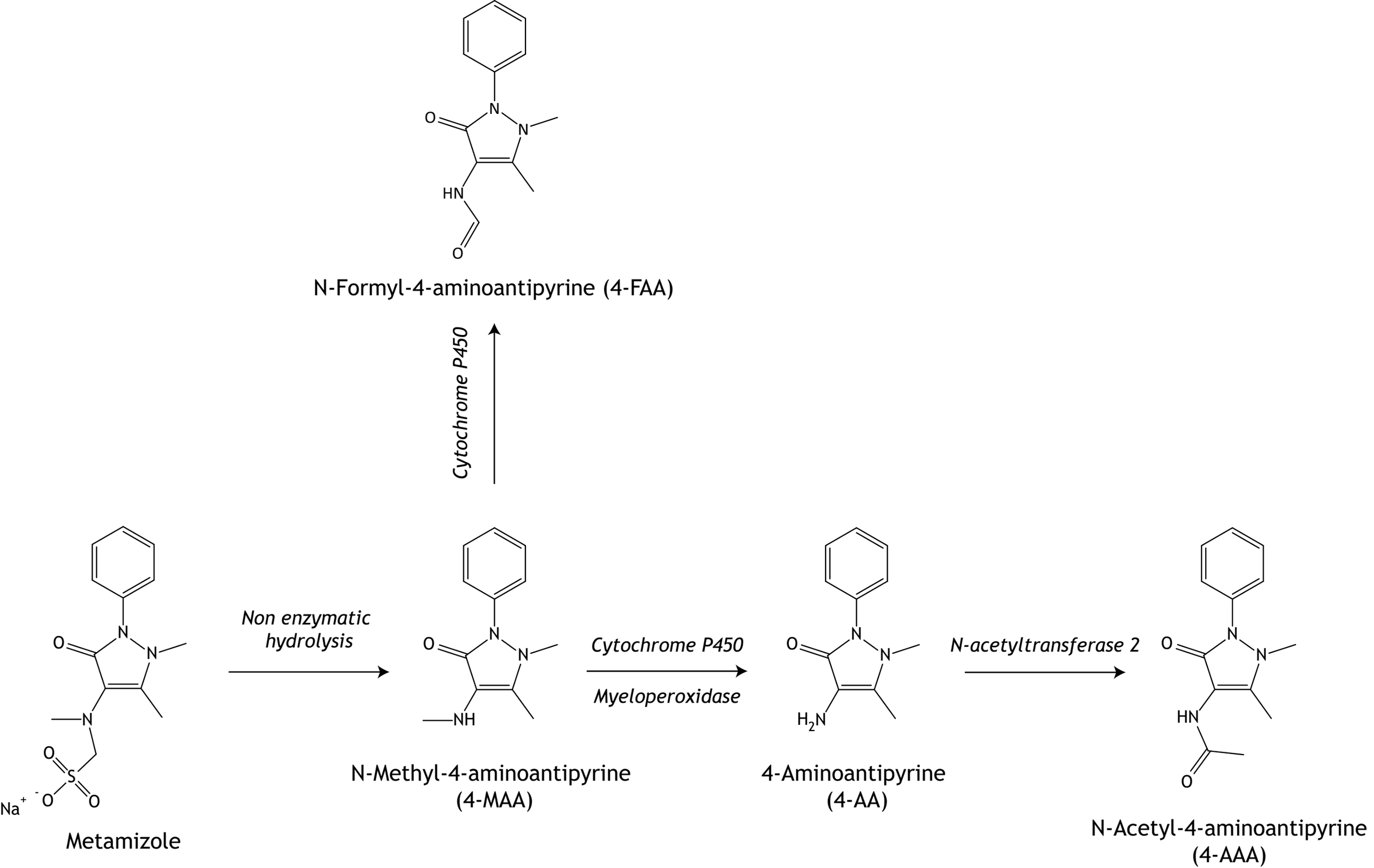
N-Formyl-4-aminoantipyrine (4-FAA)
Cytochrome P450
Non enzymatic hydrolysis
Cytochrome P450
Myeloperoxidase
N-acetyltransferase 2
N-Methyl-4-aminoantipyrine (4-MAA)
4-Aminoantipyrine (4-AA)
N-Acetyl-4-aminoantipyrine (4-AAA)
Metamizole

1A2

Caffeine

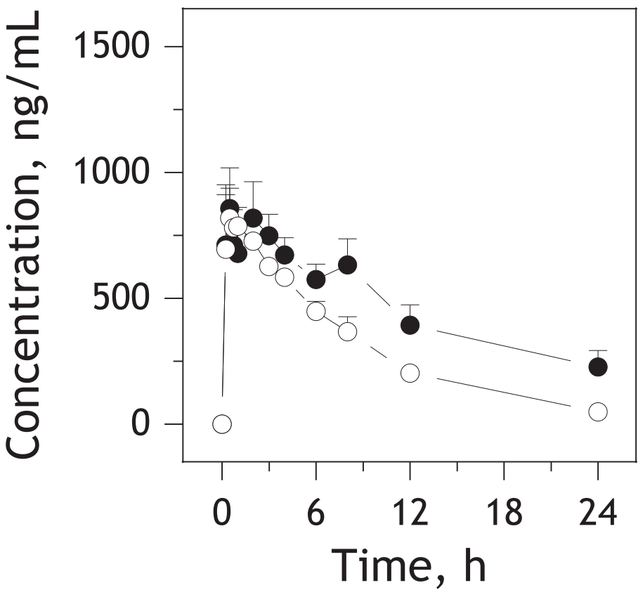

Paraxanthine

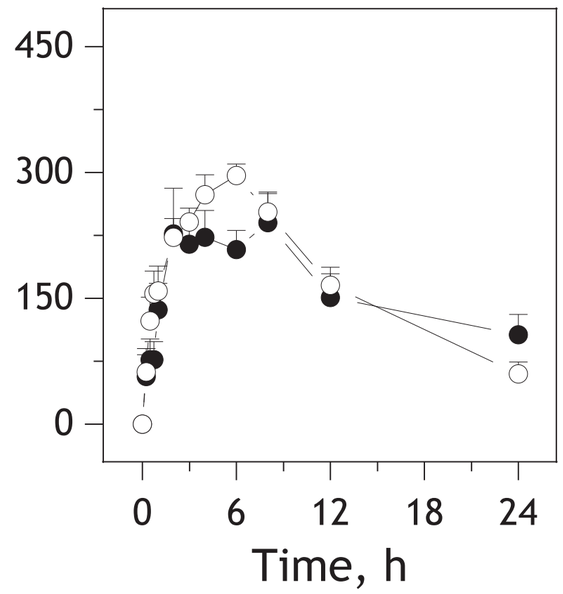

2B6

Efavirenz

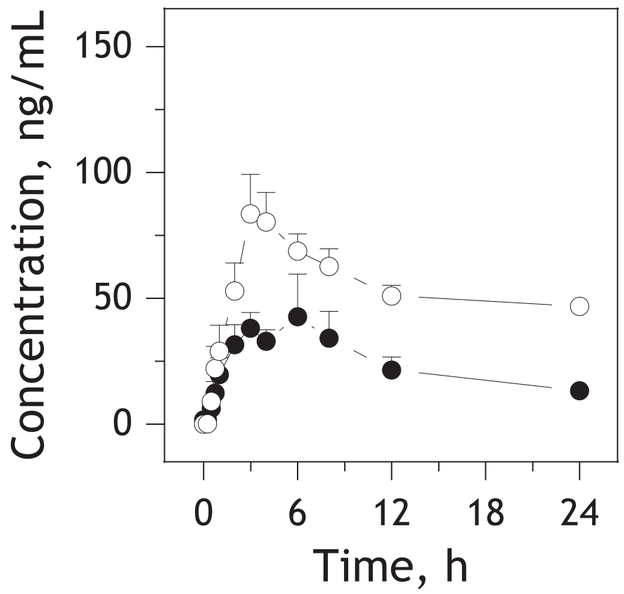

8’-Hydroxy Efavirenz

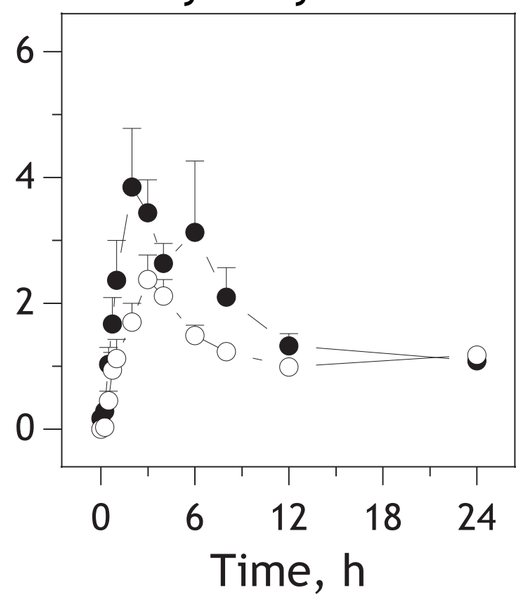

2C9

Flurbiprofen

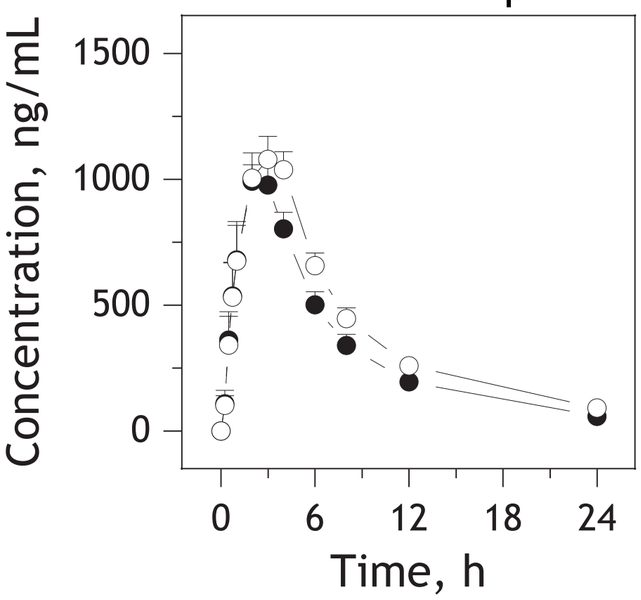

4’-Hydroxy Flurbiprofen

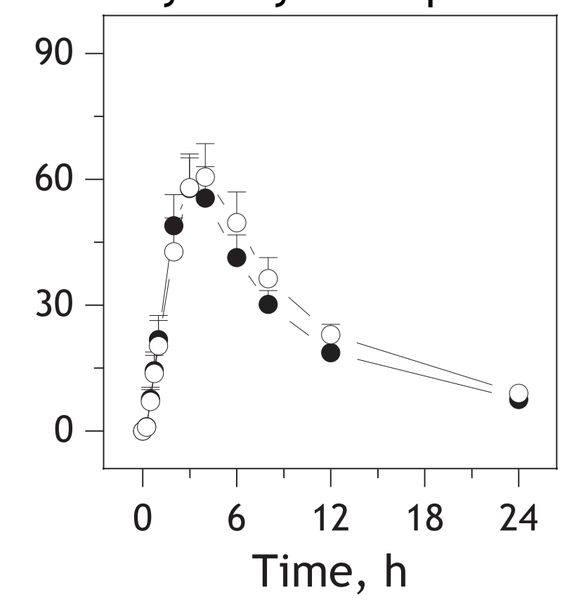

2C19

Omeprazole

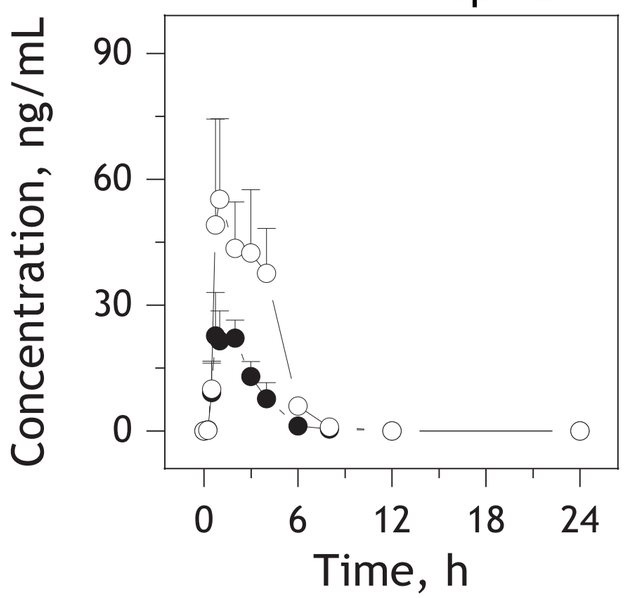

5’-Hydroxy Omeprazole

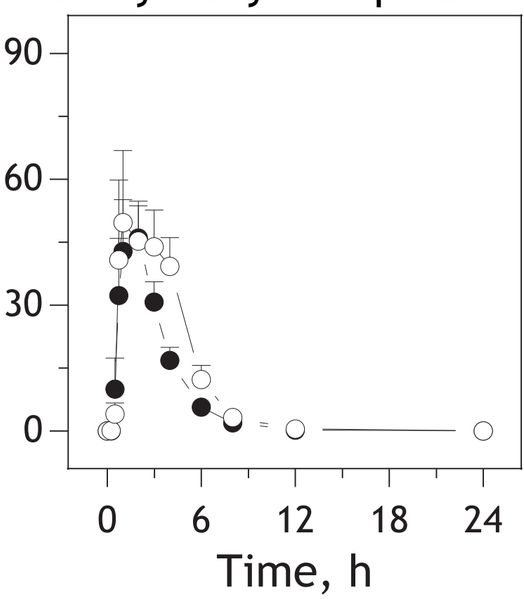

2D6

Metoprolol

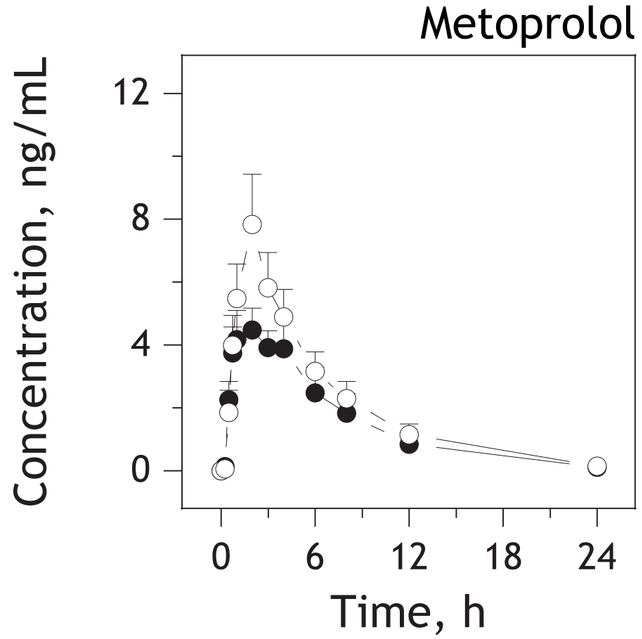

α-Hydroxy Metoprolol

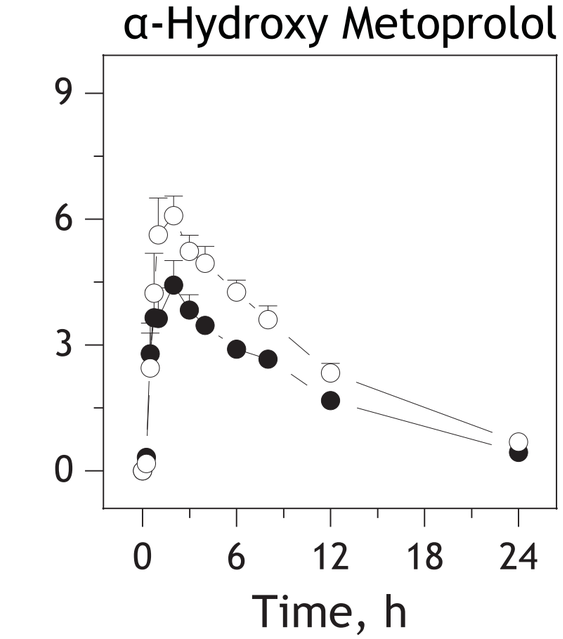

3A4

Midazolam

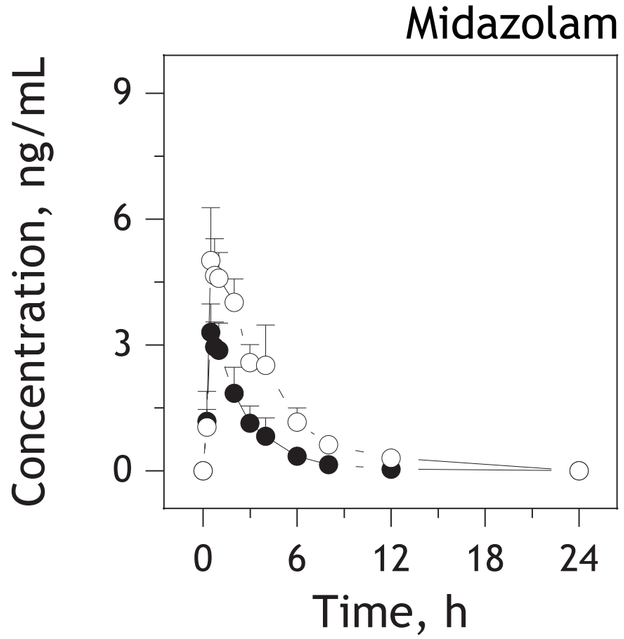

1’-Hydroxy Midazolam

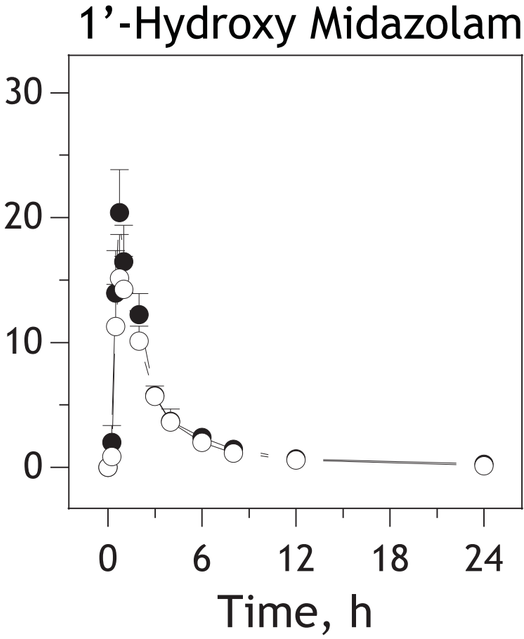

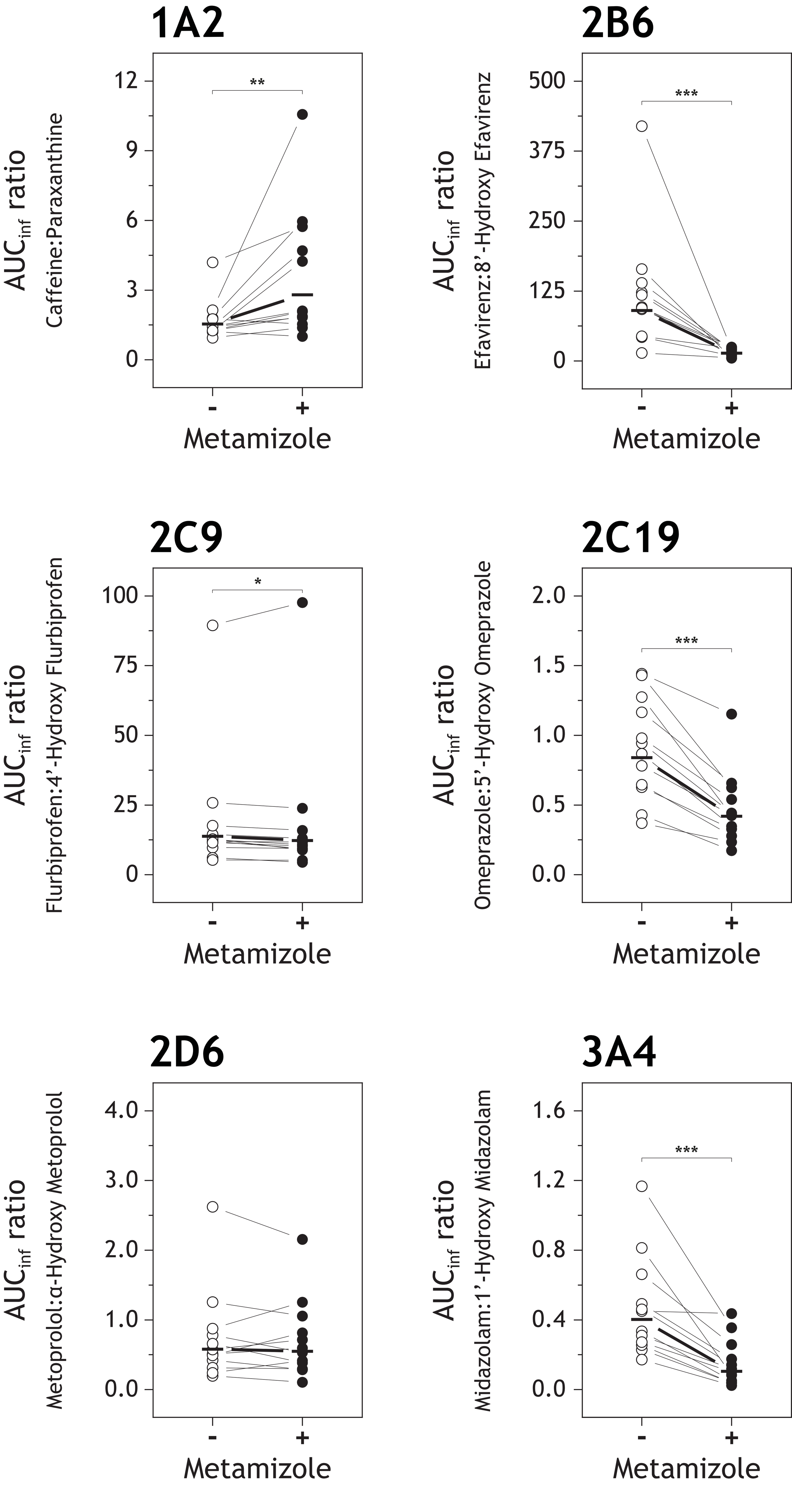
1A2
AUCinf ratio
Caffeine:Paraxanthine
12
9
6
3
0
**
-
+
Metamizole
2B6
AUCinf ratio
Efavirenz:8'-Hydroxy Efavirenz
500
375
250
125
0
***
-
+
Metamizole
2C9
AUCinf ratio
Flurbiprofen:4'-Hydroxy Flurbiprofen
100
75
50
25
0
*
-
+
Metamizole
2C19
AUCinf ratio
Omeprazole:5'-Hydroxy Omeprazole
2.0
1.5
1.0
0.5
0.0
***
-
+
Metamizole
2D6
AUCinf ratio
Metoprolol:α-Hydroxy Metoprolol
4.0
3.0
2.0
1.0
0.0
-
+
Metamizole
3A4
AUCinf ratio
Midazolam:1'-Hydroxy Midazolam
1.6
1.2
0.8
0.4
0.0
***
-
+
Metamizole

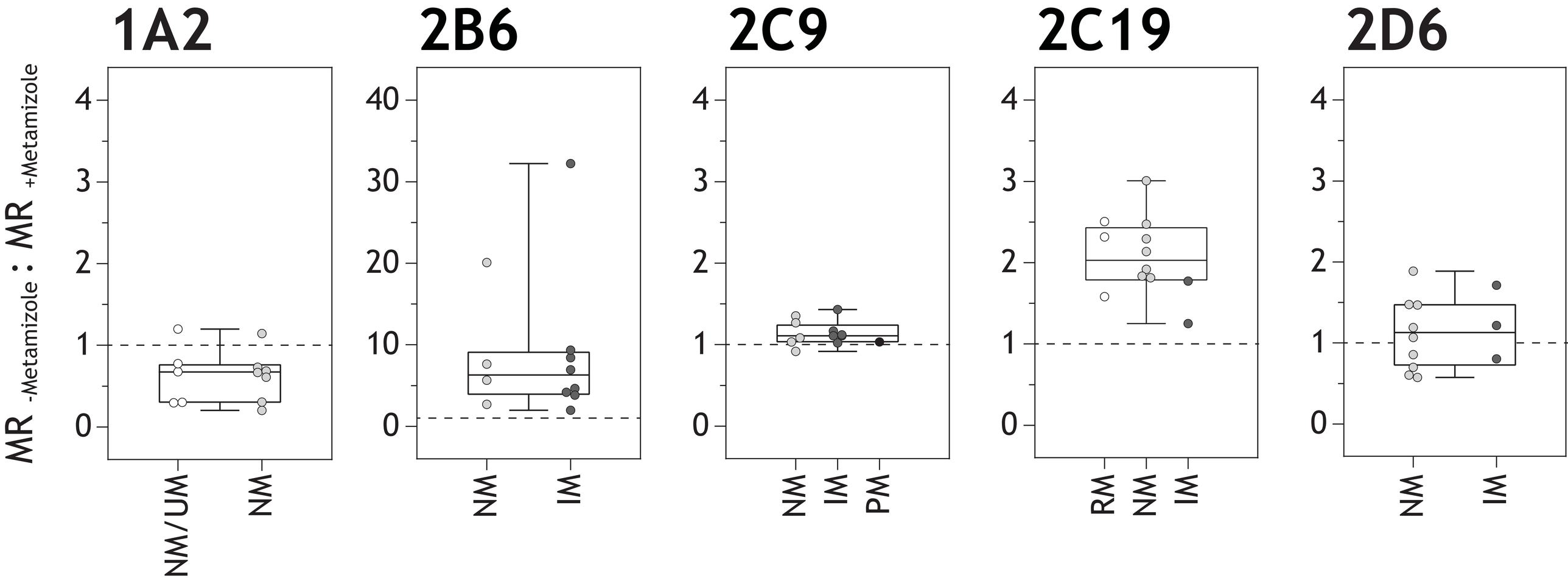
1A2
2B6
2C9
2C19
2D6
MR -Metamizole : MR +Metamizole
0
1
2
3
4
10
20
30
40
NM/UM
NM
IM
PM
RM

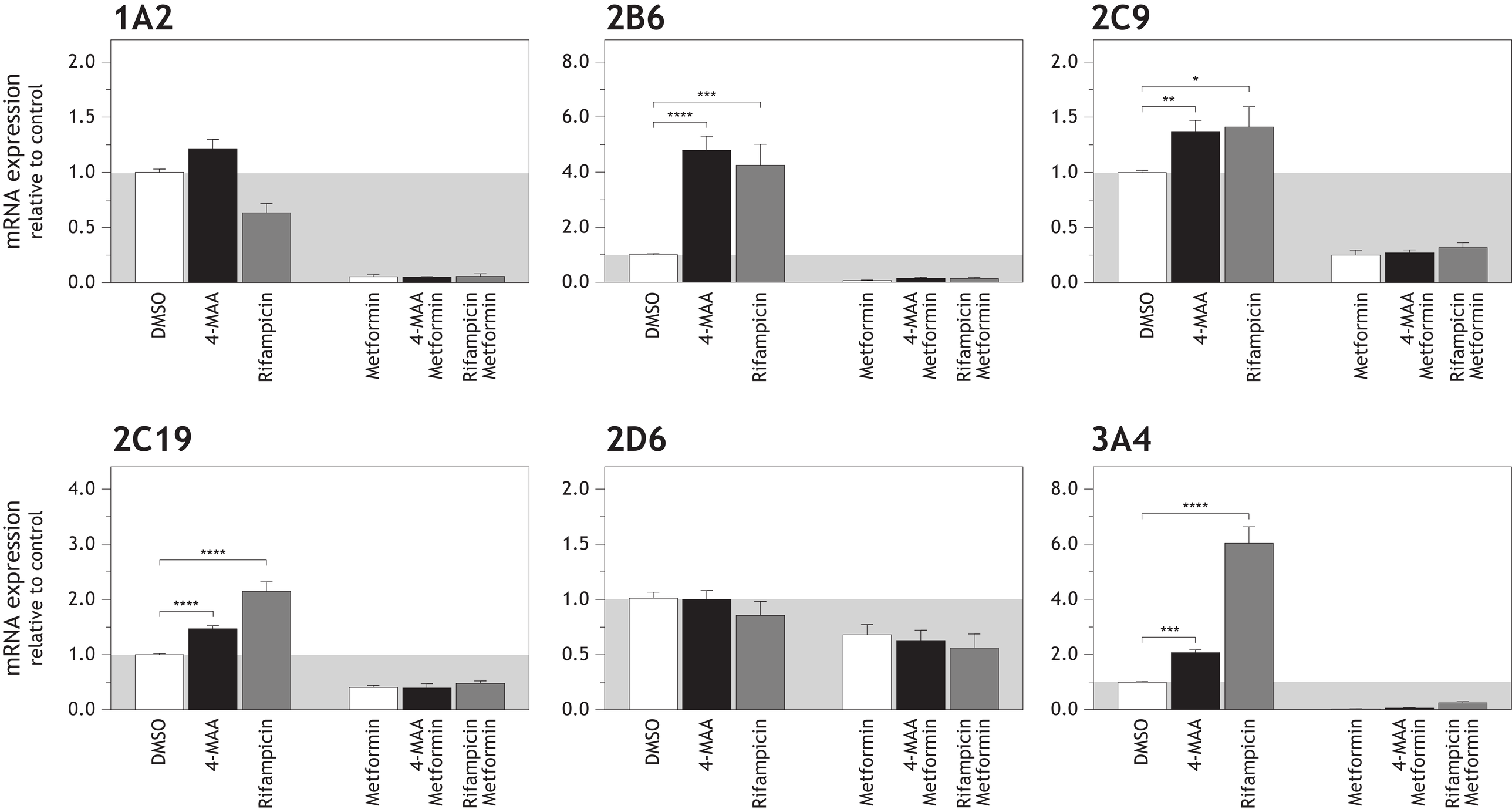
1A2
2B6
2C9
2C19
2D6
3A4
mRNA expression
relative to control
DMSO
4-MAA
Rifampicin
Metformin
4-MAA Metformin
Rifampicin Metformin
*
**
***
****

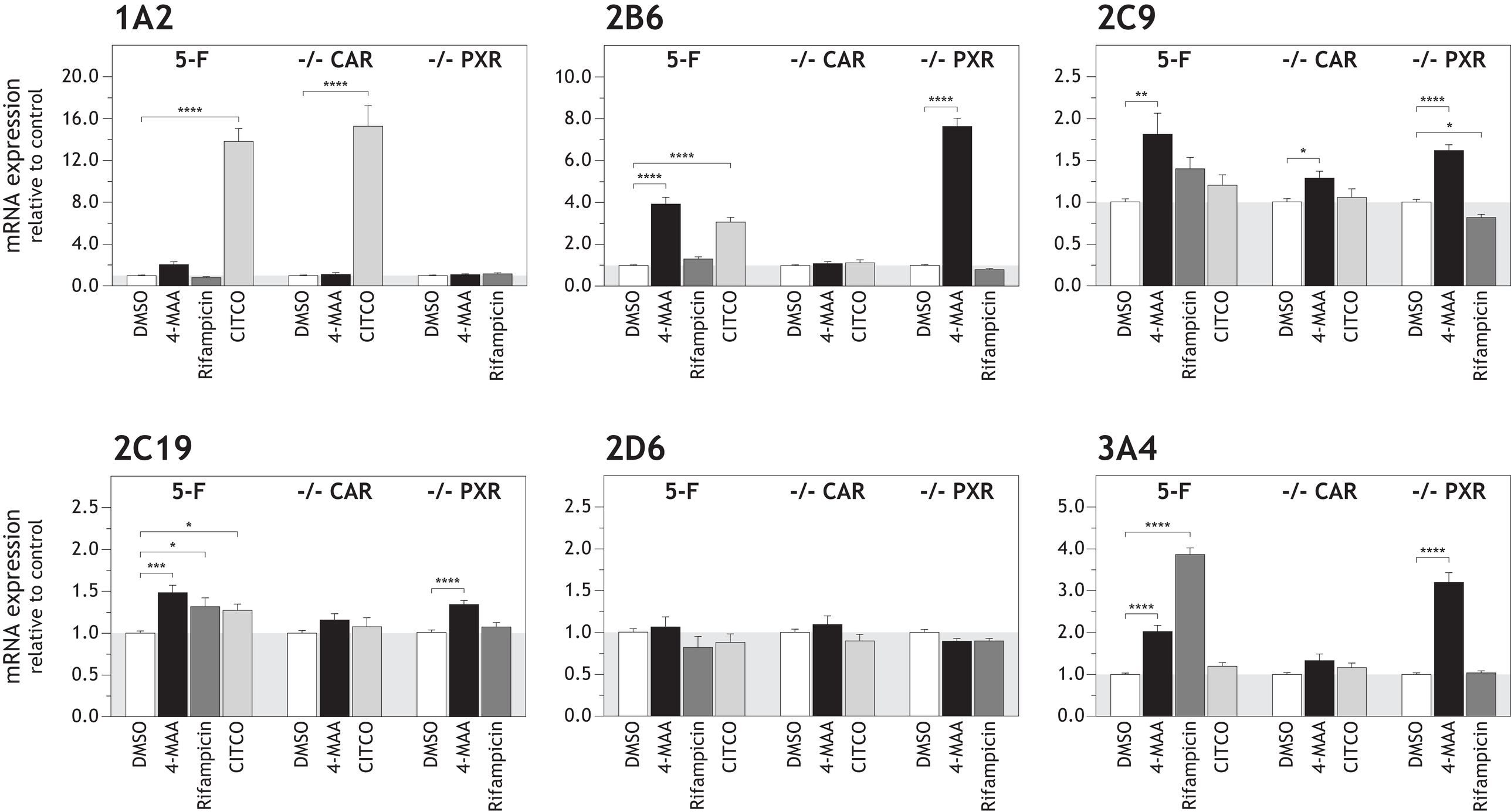
1A2
2B6
2C9
2C19
2D6
3A4
5-F
-/- CAR
-/- PXR
mRNA expression
relative to control
DMSO
4-MAA
Rifampicin
CITCO